

Mandelate Racemase in Pieces: Effective Concentrations of Enzyme Functional Groups in the Transition State[†]

Stephen L. Bearne^{*,‡} and Richard Wolfenden^{*}

Department of Biochemistry and Biophysics, University of North Carolina, Chapel Hill, North Carolina 27599-7260

Received August 16, 1996; Revised Manuscript Received November 20, 1996[®]

ABSTRACT: Mandelate racemase (EC 5.1.2.2) catalyzes the abstraction of a proton from a carbon atom adjacent to a carboxylate function, a reaction which is kinetically and thermodynamically unfavorable. Proton NMR spectroscopy and polarimetry were used to measure the rates of deuterium incorporation into the α -position of mandelate and the racemization of (*R*)-mandelate, after samples had been incubated at elevated temperatures. Using an Arrhenius plot, the value of the free energy of activation for racemization and deuterium exchange was calculated to be 34.6 (± 0.9) kcal/mol under neutral conditions, at 25 °C. This result indicates that mandelate racemase produces a remarkable rate enhancement [(1.7×10^{15}) -fold], and a level of transition state affinity ($K_{\text{TS}} = 2 \times 10^{-19}$ M), that surpasses the levels achieved by most enzymes. Methylamine, imidazole, and acetate catalyzed the nonenzymatic hydrogen–deuterium exchange reaction at 170 °C, and the values of the second-order rate constants are $2.8 (\pm 0.2) \times 10^{-5}$, $13.4 (\pm 0.7) \times 10^{-5}$, and $\leq 4 (\pm 1) \times 10^{-7} \text{ M}^{-1} \text{ s}^{-1}$, respectively. By comparing wild-type mandelate racemase's proficiency as a catalyst with the proficiencies of these small molecules which correspond to the missing pieces in the variant enzymes Lys166Arg [Kallarakal, A. T., *et al.* (1995) *Biochemistry* 34, 2788–2797], His297Asn [Landro, J. A., *et al.* (1991) *Biochemistry* 30, 9274–9281], and Glu317Gln [Mitra, B., *et al.* (1995) *Biochemistry* 34, 2777–2787], we estimate the effective concentrations of the catalytic side chains of Lys 166, His 297, and Glu 317 as ≥ 622 , $\geq 3 \times 10^3$, and $\geq 3 \times 10^5$ M, respectively, in the native protein. These observations support the view that general acid–general base catalysis, inefficient in simple model systems, becomes an efficient mode of catalysis when structural complementarity between an enzyme and its substrate is optimized in the transition state.

Mandelate racemase (EC 5.1.2.2) catalyzes the interconversion of the two stereoisomers of mandelic acid (Scheme 1) (Hegeman, 1970; Kenyon & Hegeman, 1979; Kenyon *et al.*, 1995). Isotope exchange and site-directed mutagenesis experiments indicate that mandelic acid racemization proceeds by a two-base mechanism, Lys 166 and His 297 abstracting the α -proton from (*S*)-mandelate and (*R*)-mandelate, respectively (Powers *et al.*, 1991; Neidhart *et al.*, 1991; Landro *et al.*, 1991). Site-directed mutagenesis experiments indicate that Glu 317 is also important for catalysis, functioning as a general acid (Mitra *et al.*, 1995). Catalysis by mandelate racemase raises a puzzling question. How can enzymes catalyze rapid carbon–hydrogen bond cleavage of carbon acids with relatively high pK_{a} values? To effect catalysis, mandelate racemase must solve two problems. First, proton abstraction from carbon acids is inherently slow (Eigen, 1964; Albery, 1982; Chiang *et al.*, 1988) so that the enzyme faces a kinetic barrier. Second, the enolate or enol intermediate formed is unstable (Chiang *et al.*, 1990; Amyes & Richard, 1996) and thus poses a thermodynamic problem for the enzyme.

Recently, Gerlt and Gassman have proposed that the high-energy intermediate formed during catalysis is an “enolic”

Scheme 1



species which is stabilized by formation of a strong “low-barrier” hydrogen bond to the γ -carboxyl function of Glu 317 (Gerlt *et al.*, 1991; Gerlt & Gassman, 1992, 1993a,b; Mitra *et al.*, 1995). Guthrie and Kluger (1993) have argued that the problem is essentially thermodynamic and that electrostatic stabilization in combination with a reduction in medium polarity may be sufficient to stabilize the inherently unstable enol or enolate species formed during catalysis. Although the relative contributions of these two effects to catalysis are not known, it is clear that mandelate racemase must be very proficient at discriminating between the substrate in the ground state and the altered substrate in the transition state, binding the latter species with greater affinity and reducing the activation barrier for the reaction [Polanyi, 1921; for a review, see Wolfenden (1976)].¹ The degree to which mandelate racemase stabilizes the transition state is unknown. Estimation of its magnitude would permit more quantitative descriptions of mandelate racemase catalysis.

In the present work, we sought to address two questions. What is the magnitude of transition state stabilization

[†] This work was supported by Grant GM18325 from the National Institutes of Health. S.L.B. is a Natural Sciences and Engineering Research Council of Canada Postdoctoral Fellow.

^{*} Corresponding authors.

[‡] Present address: Department of Biochemistry, Dalhousie University, Halifax, Nova Scotia B3H 4H7, Canada.

[®] Abstract published in *Advance ACS Abstracts*, February 1, 1997.

provided by mandelate racemase, and how susceptible is the nonenzymatic reaction to catalysis by molecules that resemble groups at the active site? The results indicate that mandelate racemase produces a remarkable level of transition state stabilization, surpassing the levels that are achieved by most enzymes. Comparison of this enzyme's catalytic proficiency with those of small molecules corresponding to the missing pieces in the variant enzymes Glu317Gln (Mitra *et al.*, 1995), Lys166Arg (Kallarakal *et al.*, 1995), and His297Asn (Landro *et al.*, 1991) allows estimation of the effective concentrations of the catalytic side chains of Glu 317, Lys 166, and His 297, respectively, in the native protein.

EXPERIMENTAL PROCEDURES

Materials. (*R*)-Mandelic acid was purchased from Aldrich Chemical Co., and no impurities were detected by proton NMR spectroscopy. All other chemicals were analytical grade and used without further purification.

Kinetic Measurements. The temperature dependence of the first-order rate constants for exchange of the α -proton of (*R*)-mandelate with deuterium in D₂O and for the racemization of (*R*)-mandelate in H₂O and D₂O was determined as follows. For experiments conducted in water, solutions contained mandelic acid (0.5 M) and potassium phosphate (0.1 M, pH 7.5). For experiments conducted in D₂O, solutions contained potassium mandelate (0.5 M) and deuterium-exchanged potassium phosphate (0.1 M, pD 7.5). In all experiments, the ionic strength was maintained at 0.93 with KCl. pH meter readings were converted to pD values using the equation of Fife and Bruice (1961).

Reactions were conducted in sealed quartz tubes (4 mm inside diameter, 1 mm thick, obtained from G. M. Associates, Inc., Oakland, Ca) (Radzicka & Wolfenden, 1995, 1996) at

temperatures ranging between 130 and 230 °C. Each tube contained 500 μ L of (*R*)-mandelic acid solution and was incubated at the appropriate temperature in a Thermolyne 47900 furnace. Tubes were removed at various time points, cooled to 4 °C, and stored at this temperature until analyzed using either proton NMR spectroscopy (Bruker AMX-500 NMR spectrometer) or polarimetry (Perkin-Elmer model 241 polarimeter).

The rate of racemization of (*R*)-mandelate in both H₂O and D₂O was determined by following the change in observed optical rotation as a function of time. Mandelate solution (400 μ L) was removed from the reaction tubes corresponding to various time points and diluted to a total volume of 2 mL with water. The first-order rate constant for (*R*)-mandelate racemization was determined from linear plots of the natural logarithm of the observed rotation (at 25 °C using sodium D light) against time.

Deuterium exchange into mandelate was determined using proton NMR spectroscopy. Mandelate solution (400 μ L) was removed from the reaction tubes corresponding to various time points and placed in an NMR tube. Standard pyrazine solution (300 μ L of a 0.75 M solution in D₂O) was then added to bring the total volume to 700 μ L. The extent of deuterium incorporation into the α -position of mandelate was calculated by comparing the loss of the integrated signal intensity of the mandelate α -proton resonance with the integral of the pyrazine signal. The observed first-order rate constant for deuterium incorporation was determined from linear plots of $\ln(\alpha\text{-proton integral})$ against time. We found that following the incorporation of deuterium at the α -position of (*R*)-mandelate using NMR spectroscopy was both more precise and more accurate than following the change in optical rotation by polarimetry. For this reason, the deuterium exchange method was employed in all experiments to determine the effect of small molecules on the rate of racemization (*vide infra*).

Effect of Small Molecules on the Hydrogen–Deuterium Exchange Rate. The effect of potassium phosphate (0.05–0.357 M), imidazole (0.1–1.0 M), potassium acetate (0–0.8 M), methylamine (0–0.8 M), and MgCl₂ (0–0.277 M) on the rate of deuterium incorporation into the α -position of mandelate was investigated at 170 °C. Solutions of (*R*)-mandelate (0.1 M) in D₂O at pD 7.5 were prepared essentially as described for the temperature dependence experiments except that one of these additional compounds was present at the concentrations indicated. Methylamine and acetate solutions were buffered at pD 7.5 with 0.01 M potassium phosphate, and magnesium solutions were buffered with 0.01 M imidazole. When the effects of imidazole and phosphate were investigated, these compounds themselves served to buffer the solution at pD 7.5. The temperature dependence of the second-order rate constant for imidazole-catalyzed deuterium exchange was determined at temperatures ranging between 130 and 190 °C.

The dependence of the rate of deuterium incorporation as a function of pD was investigated at 170 °C. Potassium acetate (0.10–0.80 M, pD 4.8), methylamine (0.01–0.80 M, pD 10.6), potassium pyrophosphate (0.01–0.10 M, pD 9.4), imidazole (0.10–0.57 M, pD 6.5; 0.10–1.00 M, pD 7.5 and 8.5), and potassium phosphate (0.10–0.90 M, pD 2.12; 0.05–0.357 M, pD 7.5; 0.05–0.185 M, pD 12.3) were used to buffer solutions of (*R*)-mandelate (0.10 M) at the pD values indicated. Mandelate (0.10–0.50 M) was used to

¹ In a recent review, it has been suggested that very strong binding of the transition state geometry may not be required, because the conventional transition state binding scheme does not take into account an enzyme's ability to preorganize bound substrates or to interfere with the ability of solvent water to retard some nonenzymatic reactions (Cannon *et al.*, 1996). Those objections appear questionable to us, in several respects. Although enzymes are expected to bind substrates in an arrangement conducive to reaction, the structural details of ES are not expected to affect transition state binding affinity, whose magnitude is based on an equation of state. Thus, the maximal free energy with which an enzyme binds the altered substrate in the transition state is evaluated by comparing the rate constant of the uncatalyzed reaction with the second-order rate constant of the enzyme-catalyzed reaction and requires no reference to the state of organization of the substrates in ES or of other intermediate species that may arise on the path to the transition state (Wolfenden, 1974; Schowen, 1978). Second, while solvent water retards the rate of some nonenzymatic reactions, solvating the ground state more effectively than the transition state, reactions of this kind are not expected to depart from expectations based on the usual scheme in which all species are assumed to remain in solvation equilibrium (Wolfenden, 1972, 1983). This scheme embraces conventional examples of "catalysis by desolvation"; nonpolar transition state analogue inhibitors have been devised for enzymes catalyzing reactions of this type [see, for example, Gutowski and Lienhard (1976)]. The formal possibility that solvent relaxation effects, rather than equilibria of solvation, might limit the rate of a nonenzymatic reaction remains to be considered. If an enzyme were to catalyze a reaction by removing this kinetic impediment, then the enzyme's transition state binding affinity might seem to be overestimated, on the basis of a simple comparison of rate constants. However, solvent water is known to relax very rapidly, and solvent relaxation effects have been observed only in fast reactions such as photolysis (Maroncelli *et al.*, 1989). Most biological reactions, like that catalyzed by mandelate racemase, proceed very slowly indeed in the absence of enzymes. It would therefore be surprising if solvent relaxation impeded the progress of biological reactions to a substantial extent in the absence of enzymes.

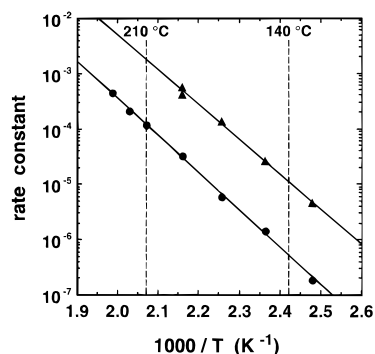


FIGURE 1: Effect of temperature on the first-order rate constant, k (s^{-1}) (●), and the second-order rate constant, k_2 ($\text{M}^{-1} \text{s}^{-1}$) (▲), for the uncatalyzed and imidazole-catalyzed exchange of deuterium into the α -position of (*R*)-mandelate, respectively, at pD 7.5. Curves shown are linear regression lines of the observed rate constant plotted as a logarithmic function of the reciprocal absolute temperature. The enthalpy and entropy of activation for the uncatalyzed and imidazole-catalyzed exchange reactions are given in Table 1.

buffer the solution at pD 3.4. The rate of deuterium incorporation into (*R*)-mandelate (0.10 M) was also measured in solutions of KOD (0.05–0.50 M) and DCl (0.10–0.50 M).

All solutions were adjusted to the desired pD value using solutions of either DCl or KOD in D_2O . Prior to use, the exchangeable protons on imidazole, methylamine hydrochloride, and potassium phosphate were replaced by deuterium by dissolution of the compound in D_2O and subsequent removal of the solvent by rotary evaporation ($\leq 60^\circ\text{C}$). This process was repeated three times. In all cases, the ionic strength was maintained at 0.93 with KCl. Solutions were incubated at 170°C for various times and analyzed using NMR spectroscopy as described above (except that the concentration of the standard pyrazine solution was 0.075 M). First-order rate constants were determined in triplicate. Average values of these rate constants were plotted as a function of the concentration of the small molecule under study, and the second-order rate constants were calculated from the slopes of the linear regression lines. Buffer-independent first-order rate constants were obtained at each pD value by extrapolation to zero buffer concentration (Jencks, 1987). Reported errors are standard deviations.

RESULTS

Activation Parameters. First-order rate constants for racemization of (*R*)-mandelate and exchange of its α -hydrogen atom with deuterium were determined at temperatures ranging from 130 to 190°C with the results shown in Figure 1. Within experimental error, the values of the rate constants for racemization (data not shown) and exchange are equal. The entropy and enthalpy of activation for the racemization of (*R*)-mandelate in H_2O and D_2O , and for the exchange of the mandelate α -hydrogen with deuterium, are shown in Table 1. Activation parameters are the same for racemization and α -hydrogen exchange, and the free energy of activation is 35 kcal/mol at 25°C . No solvent isotope effect ($> 10\%$) was detected.

Effect of Small Molecules on the Hydrogen–Deuterium Exchange Rate. Imidazole catalyzes the exchange of the α -hydrogen of (*R*)-mandelate with deuterium. The value of the second-order rate constant for buffer catalysis is $13.4 (\pm 0.7) \times 10^{-5} \text{ M}^{-1} \text{s}^{-1}$ at pD 7.5 and 170°C . The effect of temperature on the second-order rate constant is shown in

Table 1: Activation Parameters for Racemization and Exchange of the α -Hydrogen of (*R*)-Mandelate

process monitored ^a	solvent	ΔG^\ddagger ^b (kcal/mol)	ΔH^\ddagger (kcal/mol)	ΔS^\ddagger (cal $\text{mol}^{-1} \text{K}^{-1}$)
racemization	H_2O	$35 (\pm 2)$	$31.9 (\pm 0.9)$	$-9.3 (\pm 0.4)$
racemization	D_2O	$34 (\pm 1)$	$30.7 (\pm 0.7)$	$-12.7 (\pm 0.4)$
^2H exchange ^c	D_2O	$34.6 (\pm 0.9)$	$30.9 (\pm 0.4)$	$-12.6 (\pm 0.3)$
^2H exchange ^d	D_2O	$35 (\pm 4)$	$32 (\pm 2)$	$-10 (\pm 1)$
^2H exchange catalyzed by imidazole ^e	D_2O	$32 (\pm 2)$	$29 (\pm 1)$	$-11.7 (\pm 0.6)$

^a The data were obtained at pD 7.5 with an I of 0.93. ^b The free energy of activation is calculated with the temperature equal to 25°C . ^c Using first-order rate constants in 0.1 M phosphate buffer. ^d Using first-order rate constants obtained by extrapolation of imidazole catalysis plots to zero buffer concentration. ^e Activation parameters are for second-order rate constants.

Table 2: Second-Order Rate Constants for Exchange of the α -Hydrogen of (*R*)-Mandelate Catalyzed by Various Species

species and pD value	$k_2 (\times 10^{-5} \text{ M}^{-1} \text{s}^{-1})^a$
imidazole	
4.8	$14 (\pm 3)$
6.5	$18 (\pm 1)$
7.5	$13.4 (\pm 0.7)$
8.5	$4.9 (\pm 0.6)$
12.3	b
phosphate	
2.1	$2.3 (\pm 0.6)$
7.5	$1.9 (\pm 0.2)$
12.3	$27 (\pm 5)$
acetate	
2.1	$0.25 (\pm 0.02)$
4.8	$6.1 (\pm 0.6)$
7.5	$\leq 0.04 (\pm 0.01)$
methylamine	
7.5	$2.8 (\pm 0.2)$
10.6	$3.0 (\pm 0.2)$
12.3	b
MgCl_2^c	$1.87 (\pm 0.09)$
none ^c	$k_1 = 4 (\pm 1) \times 10^{-6} \text{ s}^{-1}$

^a The data were obtained at 170°C ; $I = 0.93$. ^b No buffer catalysis observed. ^c pD = 7.5.

Figure 1, and the corresponding activation parameters are given in Table 1. Increasing the pD causes a marked decrease in the value of the second-order rate constant with no catalysis being observed at pD 12.3 (Table 2 and Figure 2). These data indicate that the imidazolium ion is a more effective catalyst than neutral imidazole. The values of the first-order rate constants corresponding to pD values of 6.5, 7.5, and 8.5 are 4.0×10^{-6} , 6.5×10^{-6} , and $4.1 \times 10^{-6} \text{ s}^{-1}$, respectively.

Phosphate buffer also catalyzes α -hydrogen exchange (Figure 3A). The value of the second-order rate constant is $1.9 (\pm 0.2) \times 10^{-5} \text{ M}^{-1} \text{s}^{-1}$ at pD 7.5 and 170°C (Table 2). Extrapolation to zero buffer concentration gives a value for the observed first-order rate constant of $4.0 (\pm 0.4) \times 10^{-6} \text{ s}^{-1}$ under these conditions. At pD 12.3, the value of the second-order rate constant is increased approximately 13-fold, indicating that the phosphate trianion is the most efficient catalyst. Magnesium ion catalyzes the exchange reaction (Figure 3B) with the value of the second-order rate constant equal to $1.9 (\pm 0.1) \times 10^{-5} \text{ M}^{-1} \text{s}^{-1}$ at pD 7.5 and 170°C . The value of the observed first-order rate constant at pD 7.5, obtained by extrapolation to zero magnesium concentration, is $4.0 (\pm 0.2) \times 10^{-6} \text{ s}^{-1}$.

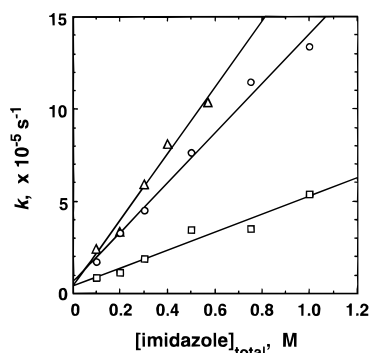


FIGURE 2: Dependence of the observed first-order rate constant for exchange of deuterium into the α -position of (*R*)-mandelate on imidazole concentration at pD values of 6.5 (Δ), 7.5 (\circ), and 8.5 (\square) at 170 °C. Reaction mixtures contained (*R*)-mandelate (0.5 M) and deuterium-exchanged imidazole (0.1–1.0 M) in D_2O ; $I = 0.93$. Second-order rate constants (Table 2) at each pD value were calculated from the slopes of the linear regression lines shown. Data at pD values 4.8 and 12.3 are not shown.

Methylamine catalyzes the exchange reaction (Figure 4), and the value of the second-order rate constant is $2.8 (\pm 0.2) \times 10^{-5} \text{ M}^{-1} \text{ s}^{-1}$ at pD 7.5 and 170 °C. Extrapolation to zero methylamine concentration gives a value for the observed first-order rate constant of $4.2 (\pm 0.8) \times 10^{-6} \text{ s}^{-1}$ at pD 7.5. No catalysis is observed at pD 12.3, indicating that the methylammonium ion is the catalyst. Acetate has little or no effect on the rate of α -hydrogen exchange at pD 7.5 (Figure 4). An upper limit for the value of the second-order rate constant for catalysis of the exchange reaction is $\leq 4 (\pm 1) \times 10^{-7} \text{ M}^{-1} \text{ s}^{-1}$. Extrapolation to zero acetate concentration at this pD value gives a value for the observed first-order rate constant of $4.51 (\pm 0.06) \times 10^{-6} \text{ s}^{-1}$. When the pD is decreased to 4.8, a 150-fold increase in the value of the second-order rate constant is observed (Table 2). However, as the pD value is decreased further to 2.1, the value of the second-order rate constant also decreases. It appears that the optimal pD value for acetate catalysis corresponds to the pD value at which mandelate is present as the anion and acetate is present as its conjugate acid.

Rate Constant for Uncatalyzed Hydrogen–Deuterium Exchange at 170 °C. The first-order rate constants, obtained by extrapolation of the buffer catalysis plots (Figures 2–4) to zero buffer concentration, can be used to calculate the first-order rate constant for the uncatalyzed deuterium exchange reaction at pD 7.5 and 170 °C. Although the observed first-order rate constants obtained from the methylamine and acetate data contain a component of catalysis due to the presence of 0.01 M phosphate used to buffer the solutions, it can be seen from Figure 3A that the effect of the phosphate is negligible. This is also true for the first-order rate constant obtained by extrapolation to zero magnesium concentration, which has a negligible contribution to the rate by the 0.01 M imidazole buffer. The first-order rate constant at 170 °C, determined in the temperature dependence study (Figure 1), is $6.0 \times 10^{-6} \text{ s}^{-1}$. This value was obtained in the presence of 0.1 M phosphate which enhanced the rate 1.5-fold at this temperature (Figure 3A). After correction for the effect of the phosphate buffer is made, a value of $4.0 \times 10^{-6} \text{ s}^{-1}$ is obtained. The average value of the first-order rate constant for the uncatalyzed exchange of the α -hydrogen of (*R*)-mandelate with deuterium at pD 7.5 and 170 °C is $4 (\pm 1) \times 10^{-6} \text{ s}^{-1}$ (Table 2).

The dependence of the observed first-order rate constant for deuterium exchange on pD is shown in Figure 5. Between pD 4 and 10, the observed first-order rate constant is pD-independent. Exchange is catalyzed by both acid and base as indicated by the ascending curves having slopes of -1 and 1 for pD values less than 1.0 and greater than 12.0. The rate of exchange can be described using the rate equation (eq 1)

$$\begin{aligned} d([2\text{-}^2\text{H}]\text{M})/dt &= k_{\text{obs}}[\text{M}]_{\text{total}} \\ &= k_{\text{D}^+}[\text{MD}][\text{D}^+] + k_{\text{non}}[\text{M}^-] + \\ &\quad k_{\text{OD}^-}[\text{M}^-][\text{OD}^-] \quad (1) \end{aligned}$$

where M^- and MD represent the mandelate anion and its conjugate acid in D_2O , respectively. The observed first-order rate constant for deuterium exchange (k_{obs}) is related to the deuterium ion concentration as shown in eq 2:

$$k_{\text{obs}} = \frac{k_{\text{D}^+}[\text{D}^+]^2 + k_{\text{non}}K_a + k_{\text{OD}^-}K_wK_a/[\text{D}^+]}{[\text{D}^+] + K_a} \quad (2)$$

where $K_w = [\text{D}^+][\text{OD}^-]$ and K_a is the dissociation constant for mandelic acid in D_2O at 170 °C. Equation 2 correctly describes the shape of the pD–rate curve shown in Figure 5. The curve has been fit to eq 2 using the following values: $k_{\text{D}^+} = 3 (\pm 1) \times 10^{-5} \text{ M}^{-1} \text{ s}^{-1}$, $k_{\text{OD}^-} = 3.3 (\pm 0.6) \times 10^{-3} \text{ M}^{-1} \text{ s}^{-1}$, $k_{\text{non}} = 4.2 (\pm 0.9) \times 10^{-6} \text{ s}^{-1}$, $K_a = 4.9 \times 10^{-3} \text{ M}$, and $K_w = 1.95 \times 10^{-15} \text{ M}^2$ (Windholz, 1983). Any attempt at a detailed interpretation of the pD–rate profile may be inappropriate, since the exact pD values of the solutions, the pK_a of mandelic acid, and the ionization constant of D_2O are not known at 170 °C. Accordingly, there is some question as to the accuracy of curve fitting, and the exact value of pD at room temperature to which the experimental points correspond. This uncertainty in the pD–rate profile does not affect the analysis presented in the present work, however. The major significance of the pD–rate profile is in showing that the nonenzymatic first-order rate constant for hydrogen–deuterium exchange, measured at pD 7.5, is pD-independent.

DISCUSSION

Nonenzymatic Racemization of Mandelate

In the absence of enzyme, racemization of mandelate is so slow that it has only been observed at elevated temperatures in the presence of concentrated acid (Campbell & Campbell, 1932; Chiang *et al.*, 1990) or alkali (Campbell & Campbell, 1932; Erlenmeyer *et al.*, 1936; Pocker, 1958). In the present work, we were able to measure rate constants for the exchange of deuterium and racemization in neutral solution. First-order rate constants for racemization of mandelate in H_2O at pH 7.5 were found to be equal, within experimental error, to first-order rate constants for racemization of mandelate in D_2O at pD 7.5. These rate constants were also equal, within experimental error, to the first-order rate constants for incorporation of deuterium into the α -position of mandelate in D_2O at pD 7.5. Thus, deuterium exchange occurs with a first-order rate constant that is equivalent to the rate constant for racemization. This observation agrees with Pocker's conclusion (Pocker, 1958) that the rate of mandelate racemization in aque-

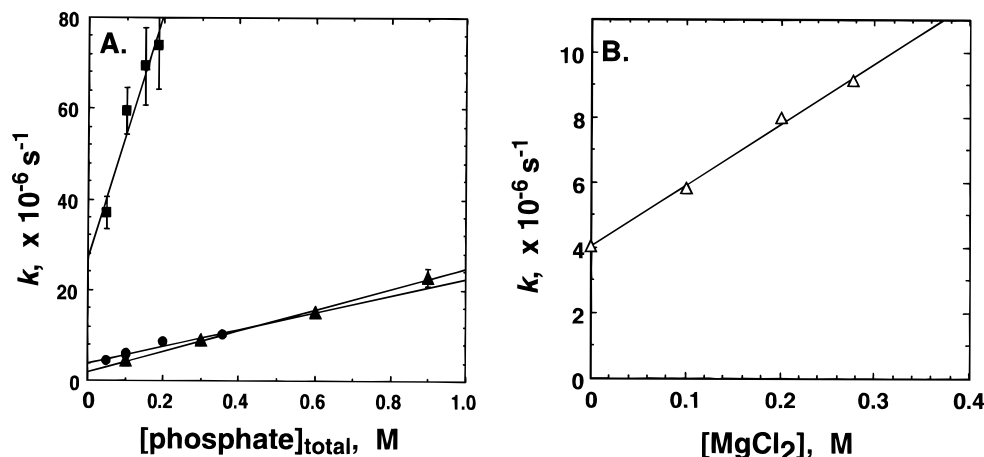


FIGURE 3: (A) Dependence of the observed first-order rate constant for exchange of deuterium into the α -position of (*R*)-mandelate on phosphate buffer concentration at pD 2.1 (\blacktriangle), pD 7.5 (\bullet), and pD 12.3 (\blacksquare) at 170 °C. Reaction mixtures contained (*R*)-mandelate (0.1 M for pD 12.3 and pD 2.1 and 0.5 M for pD 7.5) and deuterium-exchanged phosphate (0.10–0.90 M at pD 12.3, 0.05–0.357 M at pD 7.5, and 0.05–0.185 M at pD 12.3) in D_2O ; $I = 0.93$. (B) Dependence of the observed first-order rate constant for the exchange reaction on the divalent magnesium ion concentration at pD 7.5 and 170 °C. Reaction mixtures contained (*R*)-mandelate (0.5 M), MgCl_2 (0–0.277 M), and deuterium-exchanged imidazole buffer (0.01 M) in D_2O ; $I = 0.93$. Second-order rate constants (Table 2) were calculated from the slopes of the linear regression lines shown.

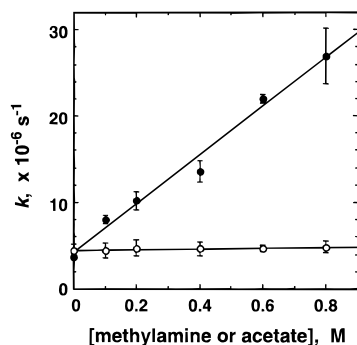


FIGURE 4: Dependence of the observed first-order rate constant for exchange of deuterium into the α -position of (*R*)-mandelate on the methylamine concentration (\bullet) and the acetate concentration (\circ) at pD 7.5 and 170 °C. Reaction mixtures contained (*R*)-mandelate (0.5 M), deuterium-exchanged phosphate buffer (0.01 M), and either deuterium-exchanged methylamine or potassium acetate (0–0.8 M) in D_2O ; $I = 0.93$. Second-order rate constants at pD 7.5 (Table 2) were calculated from the slopes of the linear regression lines shown. Data for methylamine at pD 10.6 and 12.3 and for acetate at pD 2.1 and 4.8 are not shown.

ous NaOH furnishes a measure of the rate of carbanion formation. Evidently, the ion pair, which is formed immediately upon cleavage of the carbon–hydrogen bond, separates and diffuses into the solution so rapidly that each deprotonation results in exchange (Carey & Sundberg, 1984).

The enthalpy and entropy of activation (from exchange experiments) are $30.9 (\pm 0.4) \text{ kcal/mol}$ and $-12.6 (\pm 0.3) \text{ cal mol}^{-1} \text{ K}^{-1}$, respectively. Therefore, at 25 °C, the free energy of activation for exchange (or racemization) is $34.6 (\pm 0.9) \text{ kcal/mol}$. Kresge and co-workers (Chiang *et al.*, 1990; Kresge, 1991) have studied the mandelic acid keto–enol system and determined that the $\text{p}K_{\text{E}}$ (where $K_{\text{E}} = [\text{enol}]/[\text{ketone}]$) of mandelic acid is 15.4 and the $\text{p}K_{\text{a}}$ of the enol tautomer is 6.62. These values, in combination with the $\text{p}K_{\text{a}}$ for mandelic acid, 3.41 (Jencks & Regenstein, 1968), can be used to show that at pH 7.5 mandelic acid enol lies above mandelate ion with a ΔG of 26.5 kcal/mol and that the enolate ion lies above mandelate with a ΔG of 25.3 kcal/mol (Kresge, 1991). Although the $\text{p}K_{\text{a}}$ value of the α -proton of the mandelate anion has not been measured, its value has

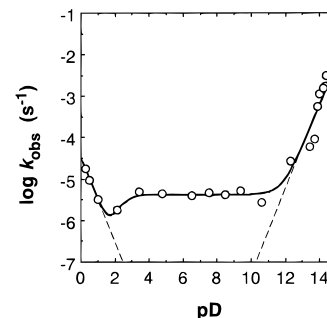


FIGURE 5: Dependence of the observed first-order rate constant for exchange of deuterium into the α -position of (*R*)-mandelate on pD at 170 °C. Experimental conditions are as described in the text. The curve shown is from a fit to the equation $k_{\text{obs}} = (k_{\text{D}^+}[\text{D}^+]^2 + k_{\text{non}}K_{\text{a}} + k_{\text{OD}^-}K_{\text{w}}K_{\text{a}}/[\text{D}^+])/([\text{D}^+] + K_{\text{a}})$. The values for k_{OD^-} , k_{D^+} , and k_{non} are $3.3 (\pm 0.6) \times 10^{-3} \text{ M}^{-1} \text{ s}^{-1}$, $3 (\pm 1) \times 10^{-5} \text{ M}^{-1} \text{ s}^{-1}$, and $4.2 (\pm 0.9) \times 10^{-6} \text{ s}^{-1}$, respectively. Dashed lines shown have slopes of -1 and 1 .

been estimated as ~ 29 (Gerlt *et al.*, 1991). The mandelate dianion therefore lies above the mandelate anion by approximately 29 kcal/mol in free energy at pH 7.5. The value of the free energy of activation determined in the present work is compatible with any of the species shown in Figure 6 [the neutral enol (1), the enolate anion (2), or the enolate dianion (3)] being an intermediate in the exchange reaction.

Transition State Stabilization by Mandelate Racemase

An upper limit can be estimated for the dissociation constant of an enzyme's complex with the altered substrate in the transition state (K_{tx}) by dividing the rate constant for the reaction in the absence of enzyme (k_{non}) by the catalytic efficiency of the enzyme ($k_{\text{cat}}/K_{\text{m}}$) [for reviews, see Wolfenden (1974, 1976)]. To determine the rate of mandelate racemization in the absence of enzyme, we measured the rate of racemization of (*R*)-mandelate and the rate of deuterium exchange with the α -hydrogen of (*R*)-mandelate in neutral solution. At 25 °C, the free energy of activation for racemization is $34.6 (\pm 0.9) \text{ kcal/mol}$, corresponding to a nonenzymatic rate constant equal to $3 (\pm 2) \times 10^{-13} \text{ s}^{-1}$. Comparison of k_{non} with the turnover number ($k_{\text{cat}} = 500$

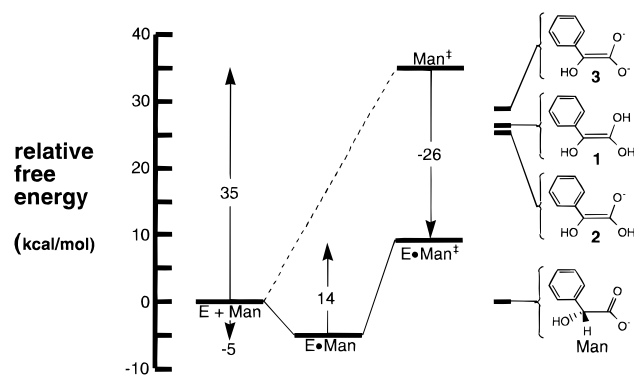


FIGURE 6: Free energy profile (pH 7.5 and 25 °C) for the racemization of (*R*)-mandelate (Man) in the absence of enzyme (dashed line) and in the presence of mandelate racemase [solid line, from Mitra *et al.* (1995)]. Man[‡] represents the altered mandelate in the transition state. The free energy of the enol (1) and enolate anion (2) are calculated from the data of Chiang *et al.* (1990) and Kresge (1991). The free energy of the enolate dianion (3) is calculated assuming that the p*K*_a value of the α-proton of mandelate is ~29 (Gerlt *et al.*, 1991).

s⁻¹) reported for the mandelate racemase-catalyzed racemization of (*R*)-mandelate (Mitra *et al.*, 1995) indicates a rate enhancement of (1.7×10^{15}) -fold at pH 7.5 and 25 °C. Comparison of *k*_{non} with the value of *k*_{cat}/*K*_m (Table 3) indicates that the upper limit of the dissociation constant of the enzyme–substrate complex in the transition state (*K*_{tx}) is approximately 2×10^{-19} M. Accordingly, mandelate racemase stabilizes the altered substrate in the transition state (ΔG_{tx}) by at least -26 kcal/mol (Figure 6).²

Many enzymes catalyze the abstraction of a proton from a carbon atom adjacent to a carbonyl/carboxylic acid group with *k*_{cat}/*K*_m values of $\approx 10^6$ – 10^8 M⁻¹ s⁻¹. This is illustrated in Table 5 for mandelate racemase, fumarase, triose-phosphate isomerase, and ketosteroid isomerase. In solution, the p*K*_a values of the α-protons of most aldehydes and ketones are ~16–20, whereas the p*K*_a values of the α-carbon atoms of most carboxylate anions are ≥ 29 (Gerlt *et al.*, 1991). To abstract a proton from a carbon atom, an enzyme must overcome both a kinetic barrier (Eigen, 1964; Albery, 1982; Chiang *et al.*, 1988) and (because the corresponding enolates are unstable) a thermodynamic barrier (Chiang *et al.*, 1990; Amyes & Richard, 1996). Hence, the nonenzymatic rate constants for conversion of glyceraldehyde 3-phosphate to dihydroxyacetone phosphate and for conversion of 5-androstene-3,17-dione to 4-androstene-3,17-dione are 6–8 orders of magnitude greater than the nonenzymatic rate constants for mandelate racemization and malate dehydration. The magnitudes of the transition state stabilization provided by mandelate racemase and fumarase are correspondingly greater than that provided by triose-phosphate isomerase or ketosteroid isomerase, by approximately 5–10 kcal/mol (Table 5).³

Catalysis by Small Molecules

To determine the susceptibility of the nonenzymatic hydrogen–deuterium exchange reaction to catalysis by small molecules, we examined the effect of imidazole, methylamine, acetate, phosphate, and magnesium ion on this reaction at 170 °C. Both methylamine and imidazole enhance the rate of deuterium exchange at pD 7.5. The variation of the value of the second-order rate constant with pD (Table 2) indicates that the conjugate acids of imidazole

and methylamine are the most efficient catalysts. Acetate, in contrast, showed little or no effect on the rate of the exchange reaction under neutral conditions. At lower pD values however, acetate enhances the rate of reaction, indicating that its conjugate acid is probably the catalyst. Phosphate also catalyzes the exchange reaction, the trianion being most effective. These findings are not unexpected, since the enolization of other carbonyl compounds has been shown to be subject to both general acid and general base catalysis (Kresge & Keeffe, 1990). Also of interest is the finding that magnesium ion catalyzes deuterium exchange, perhaps by reducing the negative charge on the carboxylate group (Guthrie & Kluger, 1993).

ΔG^S Values and Effective Molarities of Catalytic Residues at the Active Site of Mandelate Racemase

The X-ray structure of mandelate racemase isolated from *Pseudomonas putida* has been reported (Neidhart *et al.*, 1991), and several active site catalytic residues have been identified (Figure 7). The reaction catalyzed by mandelate racemase proceeds via a two-base mechanism (Powers *et al.*, 1991) in which Lys 166 abstracts the α-proton from (*S*)-mandelate (Landro *et al.*, 1994; Kallarakal *et al.*, 1995) and His 297 abstracts the α-proton of (*R*)-mandelate (Landro *et al.*, 1991). Glu 317 is believed to function as a general acid catalyst, stabilizing an enolic intermediate by a “short, strong hydrogen bond” (Mitra *et al.*, 1995). Each of these amino acids has been altered by site-directed mutagenesis, and large reductions in the values of *k*_{cat}/*K*_m have been reported (Table 3). In the present work, we determined the effect of methylamine, imidazole, and acetate on the rate of hydrogen–deuterium exchange in the absence of enzyme, using these simple molecules as models for the side chains of Lys 166, His 297, and Glu 317, each of which has been cut away in one of the variant forms of mandelate racemase.

The effective molarity of a side chain of a catalytic residue within the active site of mandelate racemase can be estimated by “cutting” the enzyme into two pieces and comparing the proficiency of the variant enzyme (*K*_{tx}^{variant}) with a truncated side chain, and the missing piece (*K*_{tx}^{piece}), measured individually, with the proficiency of the wild-type mandelate racemase or “whole” enzyme (*K*_{tx}^{wt}). The ratio *K*_{tx}^{wt}/*(K*_{tx}^{variant}*K*_{tx}^{piece}) should furnish a measure of the advantage

² If there is a difference in mechanism between the enzymatic and nonenzymatic reactions, or if the rate of the enzyme reaction is limited by some event that does not involve bond making or breaking in the substrate, then the value of *K*_{tx} represents an upper limit for the dissociation constant of the enzyme–substrate complex in the transition state (Wolfenden, 1976). In the reaction catalyzed by mandelate racemase, both proton abstraction from the substrate and reprotonation to form the product are partially rate-determining (Mitra *et al.*, 1995).

³ It should be noted that for the enzymes fumarase, triose-phosphate isomerase, and ketosteroid isomerase the value of *K*_{tx} is an upper limit since the rate-limiting process does not involve carbon–hydrogen bond making or breaking. The rate-limiting step of the fumarase-catalyzed reaction may involve product release (Blanchard & Cleland, 1980; Sweet & Blanchard, 1990), or proton exchange, accompanied by a slow conformational isomerization (Rose *et al.*, 1992, 1993). Catalysis by triose-phosphate isomerase is limited solely by the diffusion of the substrate into the active site (Blacklow *et al.*, 1988). The free energy profile for the ketosteroid isomerase-catalyzed conversion of 5-androstene-3,17-dione to 4-androstene-3,17-dione is remarkably similar to that of triose-phosphate isomerase; no single step appears to be cleanly rate-limiting so that both chemical steps and the diffusion of substrate and enzyme make significant contributions to the observed rate constant (Hawkinson *et al.*, 1991).

Table 3: Enzymatic and Nonenzymatic Kinetic Parameters for Mandelate Racemization and α -Hydrogen Exchange

variant mandelate racemase	missing piece	k_{non} (25 °C) ^a ($\times 10^{-13}$ s ⁻¹)	k_{non} (170 °C) ^b ($\times 10^{-6}$ s ⁻¹)	k_{piece} ^b ($\times 10^{-3}$ M ⁻¹ s ⁻¹)	$k_{\text{cat}}/K_{\text{m}}$ (wild type) (M ⁻¹ s ⁻¹)	$k_{\text{cat}}/K_{\text{m}}$ (variant) (M ⁻¹ s ⁻¹)
Glu317Gln ^c	acetate	3 (\pm 2)	4 (\pm 1)	≤ 0.04 (± 0.01)	1.3 (± 0.2) $\times 10^6$	42 (\pm 8)
Lys166Arg ^d	methylamine	3 (\pm 2)	4 (\pm 1)	2.8 (± 0.2)	1.4 (± 0.3) $\times 10^6$	360 (\pm 75)
His297Asn ^e	imidazole	3 (\pm 2)	4 (\pm 1)	13.4 (± 0.7)	3.3 (± 0.3) $\times 10^6$	≤ 33

^a Nonenzymatic rate constant at 25 °C obtained by extrapolation from the Arrhenius plot (Figure 1). ^b Nonenzymatic rate constant obtained at 170 °C and pD 7.5 with an $I = 0.93$. ^c $k_{\text{cat}}/K_{\text{m}}$ values for the wild type and variant enzymes are from Mitra *et al.* (1995). ^d $k_{\text{cat}}/K_{\text{m}}$ values for the wild type and variant enzymes are from Kallarakal *et al.* (1995). ^e $k_{\text{cat}}/K_{\text{m}}$ value for the wild type is from Landro *et al.* (1991); the $k_{\text{cat}}/K_{\text{m}}$ value for the variant is based on k_{cat} being less than 0.001% of the wild type k_{cat} (Kenyon *et al.*, 1995) and assuming that the K_{m} of the variant is unchanged from that of the wild type. All enzyme kinetic constants are for the conversion of (R)-mandelate to (S)-mandelate.

Table 4: Free Energy Changes for Transition State Stabilization and Effective Molarities of Active Site Catalytic Residues

variant mandelate racemase	$\Delta G_{\text{tx}}^{\text{wt}}$ (kcal/mol) ^a	$\Delta G_{\text{tx}}^{\text{variant}}$ (kcal/mol) ^a	$\Delta G_{\text{tx}}^{\text{piece}}$ (kcal/mol) ^a	ΔG^{S} (kcal/mol) ^b	effective molarity (M) ^c
Glu317Gln	-25.3	-19.2	≥ 1.4	≥ 7.5	$\geq 3 \times 10^5$
Lys166Arg	-25.4	-20.5	-1.1	≥ 3.8	≥ 622
His297Asn	-25.9	≥ -19.1	-2.1	≥ 4.7	$\geq 3 \times 10^3$

^a Free energy changes are for the association of the species indicated and the altered mandelate in the transition state. ^b $\Delta G^{\text{S}} = \Delta G_{\text{tx}}^{\text{variant}} + \Delta G_{\text{tx}}^{\text{piece}} - \Delta G_{\text{tx}}^{\text{wt}}$. ^c Effective molarity = $\exp(\Delta G^{\text{S}}/RT)$.

Table 5: Transition State Stabilization by Enzymes Catalyzing Proton Abstraction from Carbon Acids

enzyme	reaction	pK _a of substrate	$k_{\text{cat}}/K_{\text{m}}$ (M ⁻¹ s ⁻¹) ^d	k_{non} (s ⁻¹) ^e	ΔG_{tx} (kcal/mol) ^f
mandelate racemase	(R)-mandelate \rightarrow (S)-mandelate	$\sim 29^a$	1.3×10^6	3.0×10^{-13}	-26
fumarase	(S)-malate \rightarrow fumarate	$> 22-30^b$	7.1×10^7	7.6×10^{-14}	-30
triose-phosphate isomerase	(R,S)-glyceraldehyde 3-P \rightarrow dihydroxyacetone P	$\sim 17^a$	2.4×10^8	4.3×10^{-6}	-19
ketosteroid isomerase	5-androstene-3,17-dione \rightarrow 4-androstene-3,17-dione	12.7 ^c	3.0×10^8	1.7×10^{-7}	-21

^a Gerlt *et al.* (1991). ^b Approximation; cf. Gerlt *et al.* (1991). ^c Zeng and Pollack (1991). ^d Enzyme kinetic parameters were obtained for mandelate racemase from Mitra *et al.* (1995), for fumarase from Bearne and Wolfenden (1995), for triose-phosphate isomerase from Putman (1972), and for ketosteroid isomerase from Pollack *et al.* (1989). ^e Nonenzymatic reaction rate constants were obtained for mandelate racemase from this study, for fumarase from Bearne and Wolfenden (1995), for triose-phosphate isomerase from Hall and Knowles (1975), and for ketosteroid isomerase from Hawkinson *et al.* (1991). ^f Free energy changes are for association of the indicated enzyme and the altered substrate in the transition state. These values were calculated using the equation $\Delta G_{\text{tx}} = RT \ln[k_{\text{non}}/(k_{\text{cat}}/K_{\text{m}})]$ (see footnote 2).

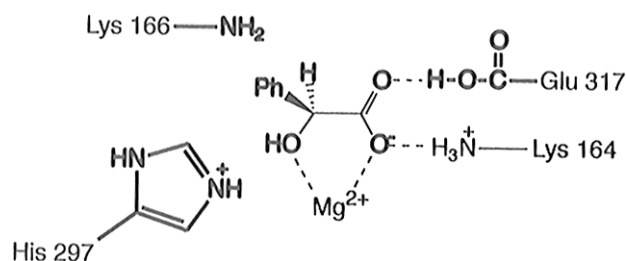


FIGURE 7: Schematic representation of the active site of mandelate racemase showing the active site residues Lys 166, His 297, and Glu 317 and the substrate (S)-mandelate [based on Neidhart *et al.* (1991) and Mitra *et al.* (1995)].

that is gained by combining the two pieces within a single molecule. The approach used to calculate the effective molarity of the Lys 166, His 297, and Glu 317 side chains at the active site of mandelate racemase is outlined below. (Please refer to the Appendix for a more detailed description of this analysis.)

Division of the value of the observed first-order rate constant for uncatalyzed exchange at 170 °C by the observed second-order rate constant for the buffer-catalyzed exchange (k_{piece} in Table 3) yields the value of $K_{\text{tx}}^{\text{piece}} [=k_{\text{non}}^{(170\text{ °C})}/k_{\text{piece}}]$ for these species at 170 °C. Since the enthalpy of activation is approximately the same for both the imidazole-catalyzed and uncatalyzed exchange reactions (parallel lines in Figure 1), the ratio $k_{\text{non}}^{(170\text{ °C})}/k_{\text{piece}}$ is expected to be essentially the same at 25 °C. The values of $K_{\text{tx}}^{\text{piece}}$ can then be converted into free energy values, and these values are

shown in Table 4. K_{tx} values for wild-type mandelate racemase and variant proteins are calculated by dividing the rate constant for racemization in the absence of enzyme (k_{non} at 25 °C, Table 3) by the catalytic efficiency of the desired enzyme species ($k_{\text{cat}}/K_{\text{m}}$). These values can be converted to free energies of transition state stabilization, and the results are presented in Table 4. The connection free energy (ΔG^{S}) is calculated using the free energies of transition state stabilization provided by wild-type mandelate racemase, the variant forms of mandelate racemase, and the corresponding active site pieces (see the Appendix and Table 4).

Thus, the energetic advantages that mandelate racemase gains by having the side chains of the catalytic residues Lys 166, His 297, and Glu 317 covalently attached within the active site are ≥ 3.8 , ≥ 4.7 , and ≥ 7.5 kcal/mol, respectively. The corresponding “effective concentrations” of the reactive side chains of Lys 166, His 297, and Glu 317 are ≥ 622 , $\geq 3 \times 10^3$, and $\geq 3 \times 10^5$ M, respectively.

Caveats

(A) *Mechanism and Ionization States.* Any or all of the three reactions, used for comparison with that of wild-type mandelate racemase to calculate the value of ΔG^{S} , could involve a mechanism differing from that of the wild-type enzyme. The expected consequences of such variation in mechanism are discussed in detail in the Appendix. Little is known about the mechanism of mandelate enolization under neutral conditions, so one can only speculate as to

how differences in mechanism might affect the present analysis of mandelate racemase catalysis. Recently, Amyes and Richard (1996) reported that the exchange of solvent deuterium with the first α -proton of ethyl acetate in D_2O is catalyzed by deuterioxide and 3-substituted quinuclidines. They found no significant exchange by a termolecular mechanism involving general acid–base catalysis of enolization [cf. Hegarty and Jencks (1975)] and concluded that deprotonation of ethyl acetate by general bases is limited by the diffusional separation of the intimate ion pair $BH^+ \cdot ^-CH_2CO_2Et$ and that the transition state for proton transfer in water strongly resembles the enolate ion. Amyes and Richard suggest that concerted formation of the enols of simple carboxylic acid derivatives is not a significant pathway for proton abstraction from such compounds in aqueous solution.

Both the observation that the variant enzymes His297Asn (Landro *et al.*, 1991) and Lys166Arg (Kallarakal *et al.*, 1995) catalyze deuterium–hydrogen exchange but not racemization and examination of the energetics of mandelate racemization using two-dimensional Marcus theory (Guthrie & Kluger, 1993) suggest that mandelate racemase catalyzes the interconversion of enantiomers by a stepwise mechanism. Gerlt and Gassman (1992) have proposed that mandelate racemase catalyzes the initial formation of an enolic intermediate by concerted general acid–general base catalysis and that this effects a substantial reduction in the activation barrier. However, Guthrie and Kluger (1993) argued that stepwise enolization with electrostatic stabilization of the enolate intermediate may be sufficient to lower the activation barrier, rendering it unnecessary to invoke concerted general acid–base catalysis. In the absence of more detailed information about the mechanism of action of mandelate racemase, it seems reasonable to assume that both variant and wild-type mandelate racemases catalyze enolization of the substrate by a stepwise mechanism, similar to that observed for nonenzymatic hydrogen–deuterium exchange.

How do the mechanisms of catalysis by acetate, methylamine, and imidazole, as “pieces”, compare with the probable mechanisms of catalysis by the corresponding amino acid side chains in wild-type mandelate racemase? Both His 297 and Lys 166 are expected to act as general base catalysts for deprotonation of mandelate (Landro *et al.*, 1991, 1994; Kallarakal *et al.*, 1995). It has also been proposed that Glu 317 functions as a general acid (Mitra *et al.*, 1995). Yet each of the reactions catalyzed by acetate, imidazole, and methylamine appears to involve general acid catalysis by the conjugate acid (or a kinetically indistinguishable combination of general base with specific acid catalysis). Although the reactions catalyzed by acetic acid and by the native enzyme may proceed by similar mechanisms, that seems less likely for the reactions catalyzed by the imidazolium or methylammonium ions. Since their mechanisms appear to differ from the mechanism of catalysis by the native enzyme, it seems likely that we have overestimated the transition state stabilization provided by these pieces. Therefore, the ΔG^\ddagger values estimated as described above represent lower limits for the effective molarities of the amino acid side chains under consideration.

One may question which state of ionization of the piece should be compared with the active site amino acid side chain. Since His 297 and Lys 166 are expected to act as general base catalysts, and Glu 317 has been proposed to

act as a general acid, it might be argued that the second-order rate constant for catalysis by the neutral forms of imidazole and methylamine, and for the conjugate acid of acetate, should be compared with the uncatalyzed rate constant. A simpler approach is to treat the piece as a separate entity that has been completely removed from the active site. With this approach, ΔG^\ddagger is expected to contain free energy contributions that include all possible modes of interaction that the side chain experiences at the active site. The ionization state of any particular piece in the active site depends on the microenvironment that it experiences and would be difficult to establish theoretically. Through comparison of the piece free in solution (and in the ionization state dictated by the pH of that solution) with the piece attached at the active site of the enzyme in the same solution, ΔG^\ddagger is expected to represent the *total* energetic advantage that mandelate racemase gains by having the amino acid side chain covalently bound at its active site, including free energy terms due to restriction of movement, electrostatics, and microenvironmental effects. At present, any attempt at more detailed dissection of ΔG^\ddagger would appear speculative.

(B) Structural Effects. Ideally, the variant enzyme of choice is one in which the side chain of an active site residue has been replaced by a methyl group. This replacement would be expected to minimize interactions that could occur if the side chain had not been sufficiently truncated. It is also possible, of course, that site-directed mutagenesis might lead to more general perturbation of the structure of the active site, resulting in increased values of ΔG^\ddagger . However, the X-ray crystal structures of mandelate racemase variants show no detectable differences in active site geometry, other than those due to simple replacement of a functional group (Landro *et al.*, 1991; Mitra *et al.*, 1995; Kallarakal *et al.*, 1995). Although small structural perturbations might escape detection by these methods, structural variations are unlikely to be a major determinant of the ΔG^\ddagger values determined in this work.

It should be noted that, while the replacement of histidine by asparagine in the His297Asn variant effectively removes a general base catalyst from the active site, this is not the case for the Lys166Arg variant. The value of k_{cat}/K_m for the Lys166Arg variant probably exceeds the value expected if the general base catalyst had been completely removed. Thus, the value calculated for the effective concentration of Lys 166 almost certainly represents an underestimate.

Catalysis and ΔG^\ddagger

One of the functions of an enzyme is to serve as an “entropy trap”, overcoming the entropic cost of gathering together free substrates from solution (Westheimer, 1962). In a similar way, the catalytic residues at the active site can be viewed as small molecules that have been already gathered from solution. Thus, an enzyme might be seen as gaining an entropic advantage by having the functional groups of catalytic residues covalently bound within its active site. The connection free energy (ΔG^\ddagger) furnishes an approximate measure of this “entropic” advantage, although these effects may not find literal expression in units of entropy, for reasons discussed above (see Appendix; Page & Jencks, 1971; Jencks, 1975, 1981).

The energetic advantage that mandelate racemase gains by having His 297 and Lys 166 covalently bound at its active

site is small compared with that gained by Glu 317. These differences in effective molarities are difficult to rationalize in the absence of precise information about the structure of the enzyme–substrate complex in the transition state. Our results imply that, relative to the ground state, the γ -carboxylate function of Glu 317 is more constrained in the enzyme–substrate complex in the transition state than either the His 297 or Lys 166 side chains. This seems reasonable considering the proposed role of Glu 317 as an electrophilic catalyst (Mitra *et al.*, 1995). The orientation that the γ -carboxylate of Glu 317 must occupy to form a hydrogen bond with the developing intermediate may be strictly defined.

What can be learned from the ground state structure? The thermal motion of the side chain atoms of His 297, Lys 166, and Glu 317 in the crystal may give some indication of the extent to which these residues are constrained. The findings of Neidhart *et al.* (1993) indicate that the average values of the temperature B factor for the side chain atoms of His 297, Lys 166, and Glu 317 are $2.8 (\pm 0.8)$, $11 (\pm 2)$, and $7 (\pm 3)$, respectively. These values do not indicate that the Glu 317 side chain is less mobile than the side chains of His 297 or Lys 166. X-ray crystal structures reveal that the distances between the α -carbon of mandelate and the ϵ -nitrogen atoms of His 297 and Lys 166 are 3.9 and 3.8 Å, respectively (Kallarakal *et al.*, 1995). The carboxylate oxygen atom of mandelate that is not coordinated to the magnesium ion is believed to be hydrogen bonded to the carboxylic acid group of Glu 317, on the basis of the 2.6–2.8 Å O–O distance between the bound substrate and the functional group (Landro *et al.*, 1994; Kallarakal *et al.*, 1995). Thus, in the ground state, Glu 317 is located closer to its site of interaction with the substrate than is His 297 or Lys 166. To the extent that the geometry of the transition state resembles that of the ground state, Glu 317 might also be expected to interact more strongly with the altered substrate in the transition state, resulting in a higher effective molarity for Glu 317 than for His 297 or Lys 166.

Comparison with the Effective Molarities in Intramolecular Acid-Catalyzed Enolization Reactions

In simple intramolecular systems, general acid–general base catalysis is typically characterized by effective molarities on the order of 1–10 M (Kirby, 1980). Values of this magnitude are too small to explain the observed rates of enzyme-catalyzed enolization reactions, as pointed out by Gerlt *et al.* (1991, 1992, 1993a,b). Such reactions may, however, be subject to unusually stringent orientation effects [see, for example, the discussion by Gandour (1981)]. Recently, Kirby and his associates demonstrated that high effective molarities can be attained in proton-transfer reactions, when the geometry supports strong hydrogen bonding (Kirby & Williams, 1994; Kirby & O'Carroll, 1994). Hydrolysis of *Z* and *E* enol ether groups in the 8-position of 1-(dimethylamino)naphthalene, for example, is catalyzed by the neighboring dimethylammonium group with an effective concentration in excess of 60 000 M (Kirby & O'Carroll, 1994).

It seems reasonable to speculate that, in enzymatic transition states, enzyme–substrate interactions are so intimate that the geometric requirements of acid–base catalysis may be met with unusual precision. Consistent with this possibility, the effective molarities that we observe for His

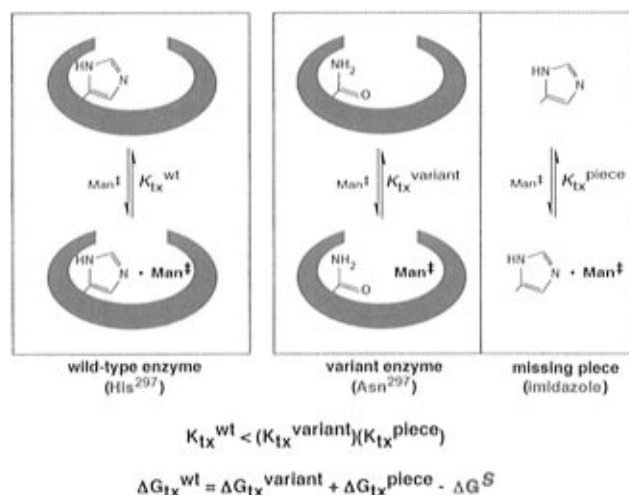


FIGURE 8: Relationship between the connection free energy (ΔG^S) and the transition state stabilization provided by wild-type mandelate racemase (ΔG_{tx}^{wt}), the variant mandelate racemase with a truncated side chain ($\Delta G_{tx}^{variant}$), and the piece that corresponds to the side chain remnant (ΔG_{tx}^{piece}). The free energy changes associated with transition state stabilization correspond to the association of a particular enzyme species or piece with the altered mandelate in the transition state (Man^\ddagger).

297, Lys 166, and Glu 317 in mandelate racemase are similar in magnitude to those described by Kirby and co-workers in model systems. Our observations support the view that general acid–general base catalysis becomes an efficient mode of catalysis when structural complementarity between an enzyme and its substrate is optimized in the transition state.

APPENDIX

Connection Free Energy (ΔG^S) and Effective Molarity of Catalytic Residues at an Enzyme Active Site

The role of cooperativity (or effective concentration) of the side chains of catalytic residues within the active site of an enzyme can be estimated by cutting the enzyme into two pieces and comparing the proficiency of the variant enzyme with a truncated side chain [$K_{tx}^{variant} = k_{non}/(k_{cat}/K_m)^{variant}$], and the missing remnant ($K_{tx}^{piece} = k_{non}/k_{piece}$), measured individually, with the proficiency of the wild-type enzyme or whole enzyme [$K_{tx}^{wt} = k_{non}/(k_{cat}/K_m)^{wt}$] (Figure 8). This furnishes a measure of the advantage that is gained by combining the two pieces within a single molecule.

Using an approach analogous to that described by Jencks (1975, 1981) for the binding of ligands, the observed free energy (ΔG_{tx}^{wt}) of association of wild-type mandelate racemase with its altered substrate in the transition state at a given temperature can be divided into three parts: (i) the observed intrinsic binding energy of a variant enzyme in which an active site functional moiety has been cut away, $\Delta G_{tx}^{i(variant)}$; (ii) the observed intrinsic binding energy of the active site residue's functional moiety, $\Delta G_{tx}^{i(piece)}$; and (iii) a connection free energy, ΔG^S , that represents the change in probability of binding that results from connection of the piece with the variant enzyme to form the wild-type enzyme. These contributions are related by eq A1:

$$\Delta G_{tx}^{wt} = \Delta G_{tx}^{i(variant)} + \Delta G_{tx}^{i(piece)} + \Delta G^S \quad (\text{A1})$$

The intrinsic binding energy of a given species, X, that is

generated when an enzyme is divided into two pieces is given by eq A2:

$$\Delta G_{\text{tx}}^{\text{i(X)}} = \Delta G_{\text{tx}}^{\text{wt}} - \Delta G_{\text{tx}}^{\text{(X)}} \quad (\text{A2})$$

where $\Delta G_{\text{tx}}^{\text{(X)}}$ is the experimentally observed free energy change for the association of species X with the altered substrate in the transition state. Therefore, the connection free energy can be calculated from observed free energy changes using eq A3:

$$\Delta G^{\text{S}} = \Delta G_{\text{tx}}^{\text{variant}} + \Delta G_{\text{tx}}^{\text{piece}} - \Delta G_{\text{tx}}^{\text{wt}} \quad (\text{A3})$$

The expression for ΔG^{S} may also be written in terms of rate constants as shown in eq A4:

$$\Delta G^{\text{S}} = RT \ln[(k_{\text{cat}}/K_{\text{m}})^{\text{wt}}/(k_{\text{cat}}/K_{\text{m}})^{\text{variant}}](k_{\text{non}}/k_{\text{piece}}) \quad (\text{A4})$$

This relationship is illustrated in Figure 8 for mandelate racemase. At first glance, the connection free energy might be expected to find expression as an entropy term. However, this free energy may also include changes in enthalpy arising from solvation effects, changes of enzyme conformation, or relief of strain (Jencks, 1981).

It is convenient to think that ΔG^{S} represents the energetic advantage that the variant enzyme gains when the remnant that has been cut away is covalently linked to the active site as it is in the wild-type enzyme. Values of ΔG^{S} may therefore be used to estimate the effective molarity of catalytically active functions within the active sites of enzymes. In principle, values of ΔG^{S} can correspond to effective concentrations, or values of $K_{\text{tx}}^{\text{variant}}K_{\text{tx}}^{\text{piece}}/K_{\text{tx}}^{\text{wt}}$, and might be expected to attain values of $<1-10^8$ M, depending on the tightness of binding in the enzyme-substrate complex in the transition state (Page & Jencks, 1971; Jencks, 1981). If the true intrinsic binding energy of a species is defined as the free energy change in the absence of strain or any change in translational and rotational entropy (Jencks, 1975), then the observed values of $\Delta G_{\text{tx}}^{\text{i(X)}}$ represent lower limits, because these conditions are not likely to be met completely by any real system. Accordingly, experimental data are likely to provide only lower limits for the value of ΔG^{S} .

Effects of Variation in Mechanism. To calculate the value of ΔG^{S} , the rate constants of four reactions are compared: the apparent second-order rate constants for the reaction of the substrate catalyzed by the variant and wild-type enzymes, the first-order rate constant for the nonenzymatic reaction, and the second-order rate constant for nonenzymatic reaction catalyzed by a piece (eq A4). If any or all of the three reactions used for comparison with the wild-type enzyme involve a different mechanism from that of the wild-type enzyme, then the value of ΔG^{S} may be either underestimated or overestimated. If the uncatalyzed reaction proceeds by a different mechanism than the enzyme and piece-catalyzed reactions, then the rate constant for the observed uncatalyzed reaction (k_{non}) is larger than that which would be observed if the nonenzymatic reaction were proceeding by the same mechanism as the catalyzed reactions. This results in the value of ΔG^{S} being *overestimated*. There are two cases in which the value of ΔG^{S} may be *underestimated*. First, if both the variant enzyme and the piece proceed by a different mechanism than that followed by the wild-type enzyme and

uncatalyzed reaction, then either the observed value of $(k_{\text{cat}}/K_{\text{m}})^{\text{variant}}$ or k_{piece} must be greater than the values of the corresponding rate constants for these reactions proceeding by the same mechanism as the wild-type enzyme and uncatalyzed reaction, respectively. Second, if the variant enzyme reaction, the piece-catalyzed reaction, and the uncatalyzed reaction all proceed by a mechanism that is different from that of the wild-type enzyme, then these three reactions would be faster than if they followed the same mechanism as the wild-type enzyme. One might expect that the observed values of k_{non} and k_{piece} are affected to the same degree so that the apparent ratio, $k_{\text{non}}/k_{\text{piece}}$, will be close to its actual value. However, the value of $(k_{\text{cat}}/K_{\text{m}})^{\text{variant}}$ will be greater than that which would be expected if the variant enzyme used the same mechanism as the wild-type enzyme. This leads to an underestimation of ΔG^{S} . Finally, if the uncatalyzed reaction proceeds by a mechanism similar to the reaction catalyzed by one of the pieces (more plausibly the reaction catalyzed by the small molecule rather than by the variant enzyme), whereas the wild-type enzyme and the other piece (in this case the variant enzyme) proceed by the same mechanism, then the value of ΔG^{S} should be roughly *equal* to its real value.

REFERENCES

- Albery, W. J. (1982) *J. Chem. Soc., Faraday Trans.* 78, 1579–1590.
- Amyes, T. L., & Richard, J. P. (1996) *J. Am. Chem. Soc.* 118, 3129–3141.
- Bearne, S. L., & Wolfenden, R. (1995) *J. Am. Chem. Soc.* 117, 9588–9589.
- Blacklow, S. C., Raines, R. T., Lim, W. A., Zamore, P. D., & Knowles, J. R. (1988) *Biochemistry* 27, 1158–1167.
- Blanchard, J. S., & Cleland, W. W. (1980) *Biochemistry* 19, 4506–4513.
- Campbell, A. N., & Campbell, A. J. R. (1932) *J. Am. Chem. Soc.* 54, 4581–4585.
- Cannon, W. R., Singleton, S. F., & Benkovic, S. J. (1996) *Nat. Struct. Biol.* 3, 821–833.
- Carey, F. A., & Sundberg, R. J. (1984) *Advanced Organic Chemistry, Part A*, 2nd ed., pp 375–376, Plenum Press, New York.
- Chiang, Y., Kresge, A. J., Santaballa, J. A., & Wirz, J. (1988) *J. Am. Chem. Soc.* 110, 5506–5510.
- Chiang, Y., Kresge, A. J., Pruszyński, P., Schepp, N. P., & Wirz, J. (1990) *Angew. Chem., Int. Ed. Engl.* 29, 792–794.
- Eigen, M. (1964) *Angew. Chem., Int. Ed. Engl.* 3, 1–72.
- Erlenmeyer, H., Schenkel, H., & Epprecht, A. (1936) *Helv. Chim. Acta* 19, 1053–1056.
- Fife, T. H., & Bruice, T. C. (1961) *J. Phys. Chem.* 65, 1079–1080.
- Gandour, R. D. (1981) *Bioorg. Chem.* 10, 169–176.
- Gerlt, J. A., & Gassman, P. G. (1992) *J. Am. Chem. Soc.* 114, 5928–5934.
- Gerlt, J. A., & Gassman, P. G. (1993a) *J. Am. Chem. Soc.* 115, 11552–11568.
- Gerlt, J. A., & Gassman, P. G. (1993b) *Biochemistry* 32, 11943–11952.
- Gerlt, J. A., Kozarich, J. W., Kenyon, G. L., & Gassman, P. G. (1991) *J. Am. Chem. Soc.* 113, 9667–9669.
- Guthrie, J. P., & Kluger, R. (1993) *J. Am. Chem. Soc.* 115, 11569–11572.
- Gutowski, J. A., & Lienhard, G. E. (1976) *J. Biol. Chem.* 252, 2363–2370.
- Hall, A., & Knowles, J. R. (1975) *Biochemistry* 14, 4348–4352.
- Hawkinson, D. C., Eames, T. C. M., & Pollack, R. M. (1991) *Biochemistry* 30, 10849–10858.
- Hegarty, A. F., & Jencks, W. P. (1975) *J. Am. Chem. Soc.* 97, 7188–7189.
- Hegeman, G. D. (1970) *Methods Enzymol.* 17, 670–674.

- Jencks, W. P. (1975) *Adv. Enzymol.* 43, 219–410.
- Jencks, W. P. (1981) *Proc. Natl. Acad. Sci. U.S.A.* 78, 4046–4050.
- Jencks, W. P. (1987) *Catalysis in Chemistry and Enzymology*, pp 163–168, Dover Publications, Inc., New York.
- Jencks, W. P., & Regenstein, J. (1968) in *Handbook of Biochemistry* (Sober, H. A., Ed.) pp J150–J189, The Chemical Rubber Co., Cleveland, OH.
- Kallarakal, A. T., Mitra, B., Kozarich, J. W., Gerlt, G., Clifton, J. G., Petsko, G. A., & Kenyon, G. L. (1995) *Biochemistry* 34, 2788–2797.
- Kenyon, G. L., & Hegeman, G. D. (1979) *Adv. Enzymol.* 50, 325–360.
- Kenyon, G. L., Gerlt, J. A., Petsko, G. A., & Kozarich, J. W. (1995) *Acc. Chem. Res.* 28, 178–186.
- Kirby, A. J. (1980) *Adv. Phys. Org. Chem.* 17, 183–278.
- Kirby, A. J., & O'Carroll, F. (1994) *J. Chem. Soc., Perkin Trans.* 2, 649–655.
- Kirby, A. J., & Williams, N. H. (1994) *J. Chem. Soc., Perkin Trans.* 2, 643–648.
- Kresge, A. J. (1991) *Pure Appl. Chem.* 63, 213–221.
- Kresge, A. J., & Keeffe, J. R. (1990) in *The Chemistry of Enols* (Rappoport, Z., Ed.) pp 399–480, John Wiley & Sons, New York.
- Landro, J. A., Kallarakal, A. T., Ransom, S. C., Gerlt, J. A., Kozarich, J. W., Neidhart, D. J., & Kenyon, G. L. (1991) *Biochemistry* 30, 9274–9281.
- Landro, J. A., Gerlt, J. A., Kozarich, J. W., Koo, C. W., Kenyon, G. L., Neidhart, D. J., Fujita, S., & Petsko, G. A. (1994) *Biochemistry* 33, 635–643.
- Maroncelli, M., MacInnis, J., & Fleming, G. R. (1989) *Science* 243, 1674–1681.
- Mitra, B., Kallarakal, A. T., Kozarich, J. W., Gerlt, J. A., Clifton, J. G., Petsko, G. A., & Kenyon, G. L. (1995) *Biochemistry* 34, 2777–2787.
- Neidhart, D. J., Howell, P. L., Petsko, G. A., Powers, V. M., Rongshi, L., Kenyon, G. L., & Gerlt, J. A. (1991) *Biochemistry* 30, 9264–9273.
- Neidhart, D. J., Howell, P. L., Petsko, G. A., Powers, V. M., Rongshi, L., Kenyon, G. L., & Gerlt, J. A. (1993) entry 2MNR in the Brookhaven Protein Data Base, 1.9 Å resolution.
- Page, M. I., & Jencks, W. P. (1971) *Proc. Natl. Acad. Sci. U.S.A.* 68, 1678–1683.
- Pocker, Y. (1958) *Chem. Ind. (London)*, 1117–1118.
- Polanyi, M. (1921) *Z. Elektrochem.* 27, 143–150.
- Pollack, R. M., Zeng, B., Mack, J. P. G., & Eldin, S. (1989) *J. Am. Chem. Soc.* 111, 6419–6423.
- Powers, V. M., Koo, C. W., Kenyon, G. L., Gerlt, J. A., & Kozarich, J. W. (1991) *Biochemistry* 30, 9255–9263.
- Putman, S. J. (1972) *Biochem. J.* 129, 301–310.
- Radzicka, A., & Wolfenden, R. (1995) *Science* 267, 90–93.
- Radzicka, A., & Wolfenden, R. (1996) *J. Am. Chem. Soc.* 118, 6105–6109.
- Rose, I. A., Warms, J. V. B., & Kuo, D. J. (1992) *Biochemistry* 31, 9993–9999.
- Rose, I. A., Warms, J. V. B., & Yuan, R. G. (1993) *Biochemistry* 32, 8504–8511.
- Schowen, R. L. (1978) *Transition States of Biochemical Processes*, Chapter 2, Plenum Press, New York.
- Sweet, W. L., & Blanchard, J. S. (1990) *Arch. Biochem. Biophys.* 277, 196–202.
- Westheimer, F. H. (1962) *Adv. Enzymol.* 24, 441–482.
- Windholz, M., Ed. (1983) *The Merck Index*, p 425, Merck & Co., Inc., Rahway, NJ.
- Wolfenden, R. (1972) *Acc. Chem. Res.* 5, 10–18.
- Wolfenden, R. (1974) *Mol. Cell. Biochem.* 3, 207–211.
- Wolfenden, R. (1976) *Annu. Rev. Biophys. Bioeng.* 5, 271–306.
- Wolfenden, R. (1983) *Science* 222, 1087–1093.
- Zeng, B., & Pollack, R. M. (1991) *J. Am. Chem. Soc.* 113, 3838–3842.

BI9620722